Investigation of Surface Structures of Supported Vanadium Oxide Catalysts by UV−vis−NIR Diffuse Reflectance Spectroscopy

Xingtao Gao and Israel E. Wachs*

Department of Chemistry and Chemical Engineering, Zettlemoyer Center for Surface Studies, Lehigh University, 7 Asa Drive, Bethlehem, Pennsylvania 18015

Received: August 12, 1999; In Final Form: December 13, 1999

UV−vis−NIR diffuse reflectance spectroscopy (DRS) was applied to study the local structures of V(V) cations on various oxide supports (Al_2O_3, ZrO_2 TiO_2, Nb_2O_5, CeO_2, and SiO_2) under hydrated and dehydrated conditions. The edge energy (E_g) of the LMCT transitions of V(V) cations was used to elucidate the local structures of V(V) cations, and a correlation between the edge energy and the number of the covalent V−O−V bonds (CVB) around the central V(V) cations was established based on some V(V) reference compounds/oxides. For TiO_2, Nb_2O_5, and CeO_2 supported vanadia catalysts, the strong support absorption in the same region as the V(V) cations prevents a reliable determination of the local structure of the surface vanadium oxide species by either the LMCT band position or the edge energy. For Al_2O_3, ZrO_2, and SiO_2 supported vanadia catalysts, the average CVB number derived from the edge energy allows the assignment of the possible structure of the surface vanadium oxide species, which is a strong function of the support, environmental conditions, and vanadia surface density. The DRS results provide reliable information and new insights into the structural characteristics of the surface vanadium oxide species on these oxide supports under different environmental conditions.

Introduction

UV−vis−NIR diffuse reflectance spectroscopy (DRS) has increasingly been applied to investigate the structures of V(V)-containing oxide compounds/mixed oxides,[1,2a,3−8] V(V)-containing zeolites,[9−18,19a] and supported vanadia catalysts[2b,20−41] due to the ligand-to-metal charge transfer (LMCT) transitions of V(V) in the 20000−48000 cm^{-1} region.[42] The local structures of the V(V) cations in these materials are often associated with the band positions of the LMCT transitions.[1−6,9−16,22,25−27,.33,34,36,39−41] The LMCT transitions of V(V) cations are usually very broad and give rise to very qualitative information. However, some recent publications indicate that the edge energies (E_g) of the LMCT transitions may be more quantitative and informative for elucidating the local structures of the V(V) cations.[18,20,29,35]

In almost all the literature publications on the supported vanadia catalysts and V(V)-containing compounds/mixed oxides, only pure samples have been tested and no attention has been paid to the deviations of the DRS results due to the effect of regular reflection. The influence of regular reflection, which may be introduced by the high concentrations of absorbing materials with high absorption coefficients,[43−45] may lead to deviations from the Schuster−Kubelka−Munk equation and distortions of the DRS spectra, which can affect the reliability of the information (the band maxima and edge energies of the LMCT transitions) obtained from the DRS studies of the V(V)-containing solid oxides/catalysts. However, this effect can be minimized by diluting the samples with white standards, such as MgO, SiO_2, and Al_2O_3.[43,45] Tandon et al.[46] found that the E_g values of the pure and diluted samples were the same in most of semiconductor materials, but slight differences were also observed for some samples. In the present work, one of the research purposes is to compare the results of the pure and diluted samples to verify the conclusions obtained from pure samples in most of the literature publications.

For UV−vis−NIR DRS studies of supported vanadia catalysts in the present work, absorption from the SiO_2 and Al_2O_3 supports can be neglected as compared to the strong absorption of the V(V) cations. However, the TiO_2, ZrO_2, CeO_2, and Nb_2O_5 supports exhibit strong absorption in the UV−vis region (especially for TiO_2, CeO_2, and Nb_2O_5 whose LMCT transitions overlap with the V(V) cations). In the case of the V_2O_5/TiO_2 catalysts, some researchers extracted the information on the vanadium oxide species by subtracting the TiO_2 absorption bands from the DRS spectra of the V_2O_5/TiO_2 catalysts.[7a,11,26b] Other researchers simply employed the TiO_2 support as the baseline reference to obtain the DRS spectra of the V_2O_5/TiO_2 catalysts,[2b,28] which was expected to exhibit only the absorption of the V(V) cations.[19b] It is not known whether these two support correction methods are correct and will give rise to reliable DRS results. In the present work, the reliability of the extracted information on the vanadium oxide species from these complex systems, where both cations are strong absorbing centers in the UV−vis region, will be systematically evaluated.

The surface structures of molecularly dispersed vanadium oxide species on various oxide supports have been extensively characterized by different techniques (IR, Raman, XANES, etc.) and have been summarized in ref 47. It is generally accepted that, at low vanadia coverages, the surface vanadium oxide species are present as isolated, 4-fold coordinated VO_4 species; whereas at monolayer coverage, highly polymerized surface vanadium oxide species are present (except on the SiO_2 support where isolated VO_4 species are still dominant). However, the local structure of the surface polymerized vanadium oxide species is still under discussion. For example, under dehydrated conditions, ^{51}V NMR spectroscopy demonstrated the presence

* To whom correspondence should be addressed. E-mail: xig2@lehigh.edu; iew0@lehigh.edu.

10.1021/jp992867t CCC: $19.00
Published on Web 01/21/2000

of both VO_4 and VO_6 species at high coverages on Al_2O_3,[48] whereas EXAFS/XANES spectroscopy suggested the presence of only VO_4 species.[49] In the present paper, from the evaluation of the edge energies of reference vanadium oxide compounds, the possible assignments of the polymerized surface vanadium oxide species on different oxide supports are proposed.

The present work focuses on the molecular structures of the surface vanadium oxide species on different oxide supports under hydrated and dehydrated conditions. The importance of the edge energy obtained from the UV−vis studies will be emphasized since the E_g values can be related to the optical basicity of the oxides,[50] which is an interesting parameter for characterizing the acid−base properties of the oxide solids.[51] The effect of the polymerization degree and the ligand of the V(V) cations on the edge energy will be investigated for a better understanding of the molecular structures of the surface vanadia species on oxide supports under different environmental conditions.

Experimental Section

1. Catalyst Preparation. The supports used for this study were Al_2O_3 (Engelhard, $S_{BET} = 222$ m^2/g), ZrO_2 (Degussa, $S_{BET} = 34$ m^2/g), SiO_2 (Cabosil EH-5, $S_{BET} = 332$ m^2/g), TiO_2 (Degussa P-25, $S_{BET} = 45$ m^2/g), Nb_2O_5 (Niobium Products Co., $S_{BET} = 57$ m^2/g), and CeO_2 (SKK company, $S_{BET} = 36$ m^2/g). The supported vanadia catalysts were prepared by the incipient-wetness impregnation of 2-propanol solutions of vanadium isopropoxide ($VO(O-Pr^i)_3$, Alfa-Aesar 97% purity) on the various supports. The preparation was performed inside a glovebox with continuously flowing N_2. After impregnation, the samples were kept inside the glovebox for overnight. The samples were subsequently dried in flowing N_2 at 120 °C for 1 h and 300 °C for 1 h, and were finally calcined in flowing air at 300 °C for 1 h and 450 °C for 2 h.

2. UV−vis−NIR Diffuse Reflectance Spectroscopy (DRS). The DRS experiments were conducted on Varian Cary 5E UV−vis−NIR spectrophotometer with the integration sphere diffuse reflectance attachment. The powder samples were loaded in a quartz flow cell with a Suprasil window and were measured in the region of 200−800 or 200−2200 nm at room temperature. A halon white (PTFE) reflectance standard was used as the baseline unless otherwise notified. The spectra of hydrated samples were obtained under ambient conditions. The spectra of the dehydrated samples were obtained after the samples were calcined at 450−500 °C in flowing O_2/He for 1 h.

To minimize the effects of regular reflection and particle size, the samples were diluted with non- or weak absorbing white standards of MgO or SiO_2 or Al_2O_3. The amount of diluent used for a sample depends on the absorbance of the sample, which should result in the Kubelka−Munk function $F(R_\infty) \leq 1$ after diluting. The corresponding diluent was also used as the baseline standard. In addition, some of the supports were also used as diluent as well as standard to examine the effect of the oxide support contribution to the overall DRS spectra. Unless otherwise mentioned, the DRS spectra of the pure and diluted samples were recorded under ambient conditions.

The DRS spectra were processed with Bio-Rad Win-IR software, consisting of calculation of $F(R_\infty)$ from the absorbance. The edge energy (E_g) for allowed transitions was determined by finding the intercept of the straight line in the low-energy rise of a plot of $[F(R_\infty)h\nu]^2$ against $h\nu$, where $h\nu$ is the incident photon energy.[44]

TABLE 1: Surface Densities of the Supported Vanadia Catalysts

catalysts	V_2O_5 wt %[a]	surface density (V atoms/nm^2)
1% V_2O_5/SiO_2	0.9	0.2
12% V_2O_5/SiO_2[b]	11.7	2.6
1% V_2O_5/Al_2O_3	1.36	0.4
5% V_2O_5/Al_2O_3	6.92	2.2
10% V_2O_5/Al_2O_3	14.05	4.9
20% V_2O_5/Al_2O_3[b]	23.72	9.3
1% V_2O_5/ZrO_2	0.43	0.8
4% V_2O_5/ZrO_2[b]	3.97	8.1
1% V_2O_5/TiO_2	1.25	1.9
5% V_2O_5/TiO_2[b]	5.89	9.2
1% V_2O_5/Nb_2O_5	1.21	1.4
5% V_2O_5/Nb_2O_5[b]	6.12	7.6
1% V_2O_5/CeO_2	1.16	1.9
4% V_2O_5/CeO_2[b]	4.77	9.2

[a] Actual V_2O_5 concentration obtained by atomic absorption. [b] Monolayer coverage as determined by Raman spectroscopy.

TABLE 2: Edge Energies of the Diluted and Pure V-Containing Compounds/Support Materials

sample	E_g (eV) (diluted)	E_g (eV) (pure)	ΔE_g[a] (eV)
$V_2O_5 + MgO$	2.32	2.31	−0.01
$Na_6V_{10}O_{28} + SiO_2$	2.23		
$MgV_2O_6 + MgO$	2.80	2.83	0.03
$NH_4VO_3 + MgO$	3.11	3.18	0.07
$Mg_2V_2O_7 + MgO$	3.42	3.50	0.08
$Mg_3V_2O_8 + SiO_2$	3.48	3.48	0.00
$Na_3VO_4 + MgO$	3.46	3.92	0.47
$TiO_2 + MgO$	3.56	3.60	0.04
$ZrO_2 + MgO$	5.24	5.23	−0.01
$Nb_2O_5 + MgO$	3.42	3.73	0.31
$CeO_2 + MgO$	3.08	3.13	0.05

[a] ΔE_g (eV) = E_g(pure) − E_g(dilut.)

Results

1. Bulk Compositions and Surface Densities. The bulk compositions and surface densities of the supported vanadia catalysts are listed in Table 1. Monolayer surface coverage for V_2O_5/SiO_2 is ∼2.6 V atoms/nm^2,[29a] and monolayer coverage for other catalysts is 7.6−9.3 V atoms/nm^2, which are consistent with previous results.[47c] These monolayer catalysts were confirmed by Raman spectroscopy since no V_2O_5 crystallites were detected.

2. Comparison of Pure and Diluted Reference Compounds. To examine the possible influence of regular reflection that is associated with the high concentrations of absorbing materials, the pure and diluted V(V)-containing reference compounds and the supports that possess LMCT transitions in the UV−vis region are compared in Table 2. Although SiO_2 and MgO as diluents give rise to similar results, MgO was used in most cases in this work since it is difficult to make homogeneous mixture of SiO_2 with other materials. The results showed that the E_g values for most of the diluted samples are almost the same as for the pure phases (within 0.1 eV). However, the E_g values of Na_3VO_4 and Nb_2O_5 differ by 0.47 and 0.31 eV when diluted, respectively.

3. Correction of the Support Contribution. Out of the six supports used for supporting vanadium oxide, four of them possess strong absorption in the UV−vis region with edge energy in the order $ZrO_2 > Nb_2O_5 \approx TiO_2 > CeO_2$ (see Table 2). To examine the effect of the support contribution to the DRS results of the supported vanadia catalysts, the highest vanadia loading sample of 20% V_2O_5/Al_2O_3 was diluted with some

TABLE 3: Edge Energies of the 20% V_2O_5/Al_2O_3 Sample Diluted with Different Materials

sample	E_g (eV) (diluted)	E_g (eV) (pure)
20% V_2O_5/Al_2O_3 + Al_2O_3	2.55	2.83
20% V_2O_5/Al_2O_3 + MgO	2.54	2.83
20% V_2O_5/Al_2O_3 + ZrO_2	2.46	2.83
20% V_2O_5/Al_2O_3 + TiO_2	2.46	2.83
20% V_2O_5/Al_2O_3 + CeO_2	2.41	2.83

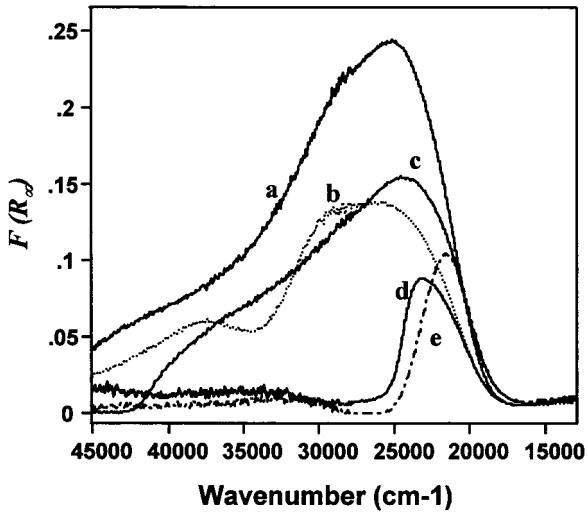

Figure 1. UV−vis DRS spectra of the 20% V_2O_5/Al_2O_3 sample diluted/referenced with (a) Al_2O_3, (b) MgO, (c) ZrO_2, (d) TiO_2, and (e) CeO_2.

supports and MgO, and the results are shown in Table 3. The edge energy of (20% V_2O_5/Al_2O_3 + Al_2O_3) mixture (Al_2O_3 as diluent) is about the same as that of (20% V_2O_5/Al_2O_3 + MgO) because both MgO and Al_2O_3 are weak and/or non-absorbers in the UV−vis region. For ZrO_2, TiO_2, and CeO_2 as diluents, the difference in the E_g values are 0.13 eV or less compared to that of Al_2O_3 or MgO as diluents. These results indicate that the edge energy is not significantly affected by the nature of the diluent when the E_g value of the surface vanadium oxide species is lower than that of the diluent by ~1.0 eV or more. However, when the E_g value of the surface vanadium oxide species is higher or close to that of the diluent or the support, as in the case of the ($Mg_3V_2O_8$ + TiO_2) mixture, no information from the V(V) cations can be obtained.

The DRS spectral features, however, are significantly affected by the use of the diluent/standard, as shown in Figure 1. The DRS spectra of the corresponding mixtures listed in Table 3 depend largely on the edge position of the support. The DRS spectrum of the (20% V_2O_5/Al_2O_3 + CeO_2) mixture possesses the narrowest band due to its lowest edge position. Apparently, the strong absorption of the support overwhelms the absorption from the vanadium oxide species, and only the absorption that does not overlap with the support absorption can be detected. The band maxima of these mixtures also vary with the diluent. The band maximum is relatively constant for mixtures with Al_2O_3, MgO, and ZrO_2 as diluents, while the band maximum is the lowest with CeO_2 as the diluent. Therefore, in the presence of strong absorbing components, such as the oxide support, the band position/maximum is not a reliable parameter for structural assignment.

Consequently, an oxide support with strong UV−vis absorption significantly modifies the DRS spectral feature of the surface vanadium oxide species, and it is a great concern how to extract reliable information from these systems. The DRS spectra of the hydrated 5% V_2O_5/Nb_2O_5 sample, after correcting

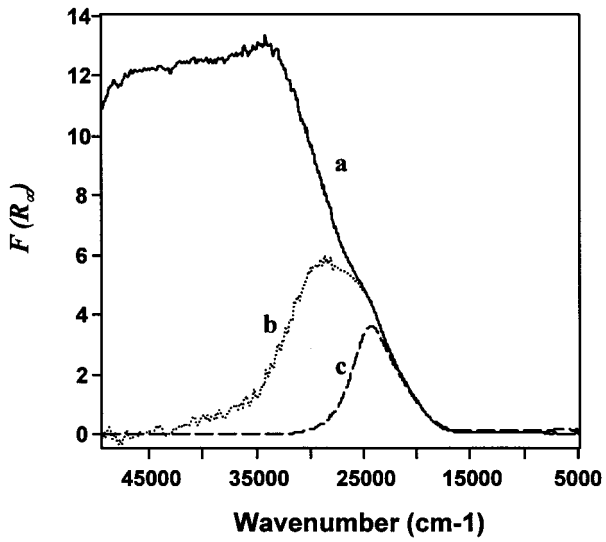

Figure 2. UV−vis−NIR DRS spectra of the hydrated 5% V_2O_5/Nb_2O_5 sample obtained (a) with PTFE as baseline, (b) after subtracting the DRS spectrum of Nb_2O_5 with PTFE as baseline, and (c) with Nb_2O_5 as baseline.

for the support contribution by using the support as the standard and by subtracting the support spectrum are compared in Figure 2. These two methods result in different spectral features. More spectra of 1% and 5% V_2O_5/Nb_2O_5 are compared in Figure 3, which were obtained under hydrated and dehydrated conditions. Note that Figure 3A exhibits only one band maximum at ~24 000 cm^{-1}, while Figure 3B shows one band maximum above 26 000 cm^{-1} with a shoulder at ~24 000 cm^{-1}. The spectral features as well as their changes in response to the environmental conditions are very consistent below 25 000 cm^{-1} in both cases, which suggests that the strong band above 26 000 cm^{-1} that appeared after subtracting the support spectrum might be artificial.

The edge energies of these samples after correcting for the support contribution by both methods are presented in Table 4, together with some TiO_2 and CeO_2 supported vanadia samples. Unlike the significant spectral difference shown above, the edge energies obtained by these two methods are very close (within 0.1 eV). This suggests that the edge energy values are relatively insensitive to the choice of the correction method, and would be more reliable for the structural assignment of the surface vanadium oxide species. Moreover, the shift of the edge energy upon hydration/dehydration was observed for all these samples.

However, it is surprising that the edge energies of the monolayer samples in Table 4, such as 5% V_2O_5/Nb_2O_5 and 5% V_2O_5/TiO_2, are only slightly lower than the lower loading samples (1% V_2O_5). This could result from the strong support absorption in the higher energy region that overlaps the weak absorption from a small amount of V(V) cations in the same wavenumbers. Another alternative explanation is that the electronic interaction with the oxide support might modify the energy gap of the surface vanadium oxide species. Therefore, because the E_g values for Nb_2O_5, TiO_2, and CeO_2 are so close to those of vanadates and vanadium oxides, the results obtained for the corresponding supported vanadium oxide species may not be reliable for the structural assignment of the surface vanadium oxide species, especially for the low vanadia loading samples.

4. Edge Energies of Supported Vanadia Catalysts. The edge energies of the pure and diluted V_2O_5/Al_2O_3, V_2O_5/SiO_2, and V_2O_5/ZrO_2 samples under hydrated and dehydrated conditions are presented in Table 5. These supports possess no support

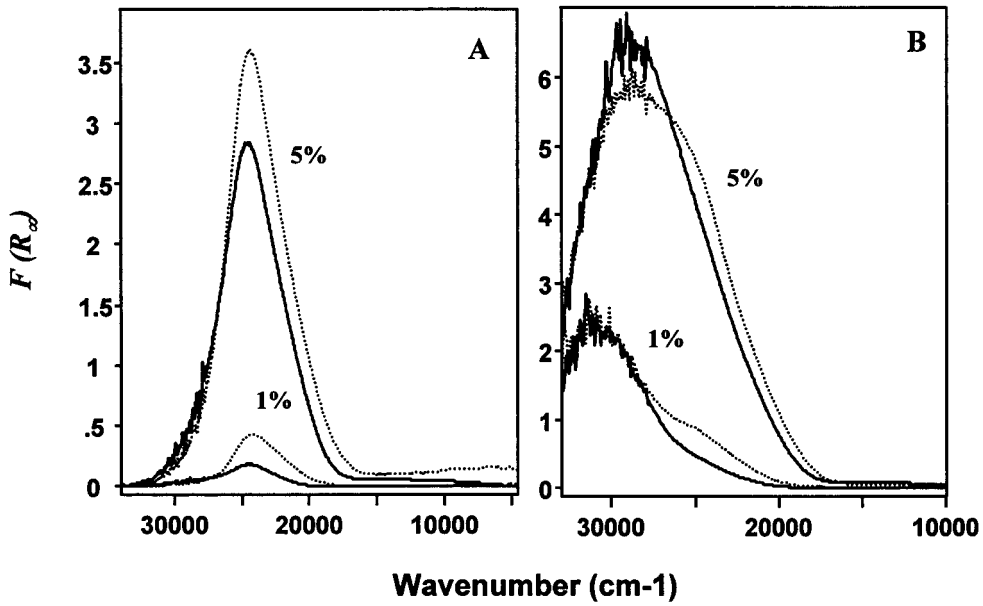

Figure 3. UV−vis−NIR DRS spectra of the 1% and 5% V_2O_5/Nb_2O_5 samples under hydrated (dotted lines), dehydrated (solid lines) conditions: (A) with Nb_2O_5 as baseline; (B) after subtracting the DRS spectrum of Nb_2O_5 with PTFE as baseline.

TABLE 4: Edge Energies of the Supported-Vanadia Catalysts Obtained after Correcting for the Support Contribution

sample	E_g (eV)[a]	E_g (eV)[b]
1% V_2O_5/Nb_2O_5 (hydr.)	2.66	2.76
1% V_2O_5/Nb_2O_5 (dehy.)	2.75	
5% V_2O_5/Nb_2O_5 (hydr.)	2.64	2.73
5% V_2O_5/Nb_2O_5 (dehy.)	2.68	2.79
1% V_2O_5/TiO_2 (hydr.)	2.74	2.72
1% V_2O_5/TiO_2 (dehy.)		2.77
5% V_2O_5/TiO_2 (hydr.)	2.65	2.65
5% V_2O_5/TiO_2 (dehy.)		2.72
4% V_2O_5/CeO_2 (hydr.)	2.50	2.62
4% V_2O_5/CeO_2 (dehy.)		2.67

[a] Using the support as the standard for the corresponding supported-vanadia catalysts. [b] After subtracting the support DRS spectra (PTFE as the standard).

TABLE 5: Edge Energies of the Diluted and Pure Supported-Vanadia Catalysts Under Hydrated and Dehydrated Conditions

sample	E_g (eV) (diluted)	E_g (eV) (pure)	ΔE_g (eV)[a]
1% $V_2O_5/Al_2O_3 + Al_2O_3$ (hydr.)	3.88	3.86	−0.02
1% $V_2O_5/Al_2O_3 + Al_2O_3$ (dehy.)	3.89	3.90	0.01
5% $V_2O_5/Al_2O_3 + Al_2O_3$ (hydr.)	3.21	3.68	0.47
5% $V_2O_5/Al_2O_3 + Al_2O_3$ (dehy.)	3.28	3.67	0.39
10%$V_2O_5/Al_2O_3 + Al_2O_3$ (hydr.)	2.86	3.27	0.41
10%$V_2O_5/Al_2O_3 + Al_2O_3$ (dehy.)	3.02	3.27	0.25
20%$V_2O_5/Al_2O_3 + Al_2O_3$ (hydr.)	2.55	2.83	0.28
20%$V_2O_5/Al_2O_3 + Al_2O_3$ (dehy.)	2.67	2.93	0.26
1% V_2O_5/SiO_2 (hydr.)		2.47	
1% V_2O_5/SiO_2 (dehy.)		3.60	
12% $V_2O_5/SiO_2 + SiO_2$ (hydr.)	2.46	2.43	−0.03
12% $V_2O_5/SiO_2 + SiO_2$ (dehy.)	3.34	3.43	0.09
1% V_2O_5/ZrO_2 (hydr.)		3.48	
1% V_2O_5/ZrO_2 (dehy.)		3.50	
4% $V_2O_5/ZrO_2 + MgO$ (hydr.)	2.80	2.78	−0.02
4% V_2O_5/ZrO_2 (dehy.)		3.13	

[a] ΔE_g (eV) = E_g(pure) − E_g(dilut.)

absorption below 40 000 cm^{-1} to affect the determination of the E_g values of the V(V) oxide species. All diluted supported vanadia samples after dehydration possess the same or lower E_g values than the pure samples. This result excludes the possibility of thermal migration of the surface vanadium oxide species from the catalysts to the corresponding oxide support diluent, since migration would decrease the surface density of the vanadium oxide species, which would result in an increase in the E_g value. The E_g values of the pure 5−20% V_2O_5/Al_2O_3 samples are higher than the diluted samples, which might be due to the effect of regular reflection that is associated with the high vanadia concentrations. However, the trend for the edge energy change upon hydration/dehydration is similar for either pure or diluted samples. The DRS spectra shown in Figure 4 also indicate that the absorption edges of the V_2O_5/Al_2O_3 samples are sensitive to the environmental conditions regardless of the possible effect of regular reflection. In addition, the E_g values in both pure and diluted states decrease systematically with increasing vanadia content/surface density. Interestingly, it is noted that the DRS spectra and the band maxima for pure V_2O_5/Al_2O_3 samples are different from the diluted samples due to the possible presence of regular reflection. The spectral resolution and band location appear to be much better when the samples were diluted.

When SiO_2 and ZrO_2 were used as the supports, only minor differences in E_g values were observed between pure and diluted samples even at monolayer coverage.

Discussion

1. Ramification of the Method for Deriving E_g Values. Several methods have been developed and applied to derive E_g values of semiconductors and amorphous solid materials from optical absorption spectra and diffuse reflectance spectra. A general power law form has been suggested by Davis and Mott,[52]

$$\alpha\hbar\omega \propto (\hbar\omega - E_g)^n$$

where α is the absorption coefficient, $\hbar\omega = h\nu$ is the photon energy, $n = 2$, 3, $^1/_2$, and $^3/_2$ for indirect allowed, indirect forbidden, direct allowed, and direct forbidden transitions, respectively. The n value for the specific transition can be determined by the best linear fit in the lower absorption region.[53,54] For V_2O_5, $CeO_2-V_2O_5$, and $B_2O_3-V_2O_5$ mixed oxides thin films, the n value of $^3/_2$ was found to be the best

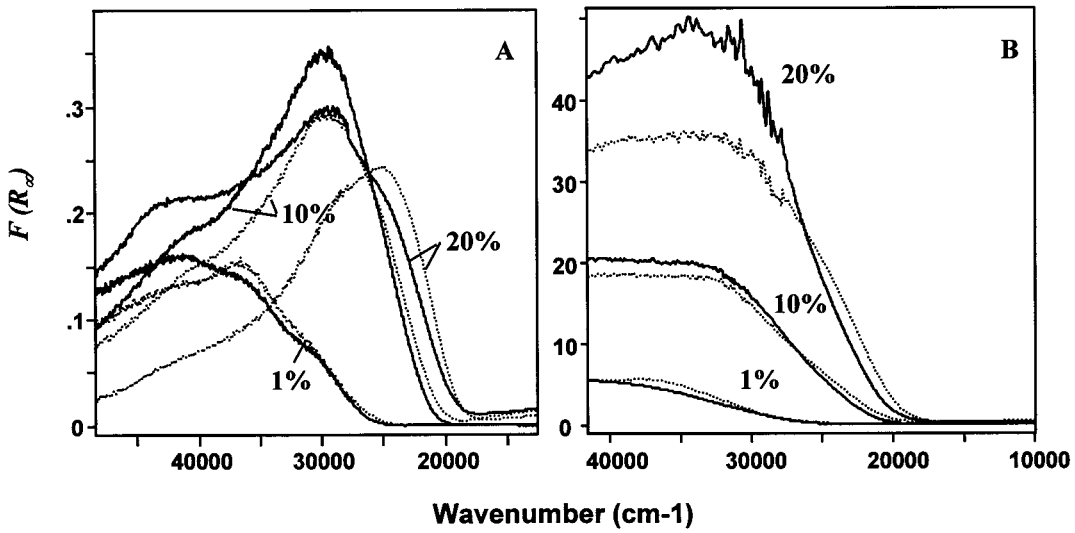

Figure 4. UV−vis−NIR DRS spectra of the 1%, 10%, and 20% V_2O_5/Al_2O_3 samples under hydrated (dotted lines) and dehydrated (solid lines) conditions: (A) diluted samples; (B) pure samples.

TABLE 6: Edge Energies Derived from Different Methods

sample	E_g (eV)[a] $n=2$	$n=3$	$n=1/2$	$n=3/2$	E_g[b] (eV)	E_g[c] (eV)
V_2O_5	2.10	1.98	2.31	2.16	2.32	2.11
$Mg_3V_2O_8$	3.08	2.87	3.48	3.20	3.48	3.10
ZrO_2	5.09	5.01	5.23	5.13	5.24	5.09
1% V_2O_5/SiO_2 (hydr.)	2.05	1.86	2.47	2.16	2.43	2.08
1% V_2O_5/SiO_2 (dehy.)	3.17	3.01	3.60	3.28	3.59	3.20
4% V_2O_5/ZrO_2 (hydr.)	2.21	1.95	2.79	2.37	2.80	2.27
4% V_2O_5/ZrO_2 (dehy.)	2.39	−	3.14	2.63	3.18	2.48

[a] Derived from the equation following Davis and Mott:[52] $[F(R_\infty)h\nu] \propto (h\nu - E_g)^n$, where $n = 2$, 3, $^1/_2$, and $^3/_2$ for indirect allowed, indirect forbidden, direct allowed, and direct forbidden transitions, respectively. [b] Derived from Tandon−Gupta's method,[46] which takes the point on the low-energy side of the curve at which the linear increase in $F(R_\infty)$ starts. [c] Derived from the equation following Tauc:[55] $[F(R_\infty)(h\nu)^2] \propto (h\nu - E_g)^2$.

fit,[53,54] which suggested a direct forbidden transition from oxygen 2p to vanadium 3d band. A similar equation was suggested by Tauc et al. for the optical absorption edge,[55]

$$\alpha\omega^2 \propto (\hbar\omega - E_g)^2$$

It appears from the literature that the choice of the specific equation is based on the best linear fit of the curve.[53,54] However, Tandon and Gupta suggested and applied another method for obtaining the forbidden energy gap.[46] The point on the low-energy side of the $F(R_\infty) \propto h\nu$ curve at which the linear increase begins was taken as the value of the forbidden energy gap. The E_g values of 15 powdered semiconductors were found to be in good agreement with the values obtained by other techniques.

To justify the method used in this study, Table 6 lists E_g values of some samples derived from all the above methods. With Davis−Mott's method, $n = 2$, $^1/_2$, and $^3/_2$ usually give nice linear fits, while $n = 3$ somehow could not give good linear fits. Both Tandon−Gupta and Tauc's methods also give rise to reasonable linear fits of the curves. However, it is difficult to find one method that is the best fit in all cases. It is interesting to note that the E_g values obtained by Davis−Mott's method with $n = {}^1/_2$ are amazingly close to the values by Tandon−Gupta's method ($\leq$0.04 eV). The E_g values obtained by the Davis−Mott method with $n = 2$ are, however, close to the values by Tauc's method. Although E_g values change with the method used, a similar trend is observed for all the samples. For example, the difference in the E_g values of the 1% V_2O_5/SiO_2 sample in the hydrated and dehydrated states for any method is between 1.12 and 1.16 eV. The results indicate that the choice of the method for deriving the E_g values is not very important for the purpose of comparison and the E_g values of different samples can be compared on a relative scale. However, in the present work the use of Davis−Mott's method with $n = {}^1/_2$ results in a E_g value of 2.31 eV for V_2O_5, which is consistent with most of the reported literature values of 2.3-2.4 eV.[56−60]

2. Correlation of Edge Energy and Local Structures of V(V) Oxides. It has been observed[29a] that the edge energy of the V(V) cations is affected by (i) polymerization degree of the V(V) cations, (ii) coordination geometry/number around the central V(V) cation, and (iii) the ligands, i.e., the cations in the second coordination sphere around the V(V) cation. The edge energy has been correlated either to the number of vanadium atoms in the second coordination sphere (CN_2) of the central V(V) cation[20] or to the local symmetry that is represented as the domain size described as an average bond distance of all the V−O bonds around the central V(V) cations.[18] However, the first proposed correlation seems to over-count the V atoms in the second coordination sphere by including the weakly bonded V−O···V bonds (bond length > 4 Å), such as the V═O···V bond between the V_2O_5 layers. Thus, it is unable to establish a good correlation for the data in the present work since the data point for V_2O_5 ($CN_2 = 7$) is far out of the linear range. The second type of correlation between the domain size (average V−O bond length) and edge energy only accounts for the local symmetry of the V(V) cation, and the edge energy is proposed to be inversely correlated with the domain size.[18] For example, the domain sizes for isolated and polymerized VO_4 units are about the same, and the domain size for V_2O_5 with square pyramidal structure is lower than that of VO_6 units.[18] This correlation did not consider the polymerization of the V(V) cations and cannot explain why MgV_2O_6 with VO_6 coordination possesses a higher edge energy than V_2O_5 with square pyramidal coordination, and NH_4VO_3 with polymerized VO_4 units possesses a lower edge energy than Na_3VO_4 and $Mg_3V_2O_8$ with isolated VO_4 units. For V(V) cations, the coordination number does not appear to be the major factor that affects the edge energy, as in the case of Ti-containing compounds.[61]

In the present work, a better empirical correlation between the edge energy (E_g) and the number of covalent V−O−V bonds

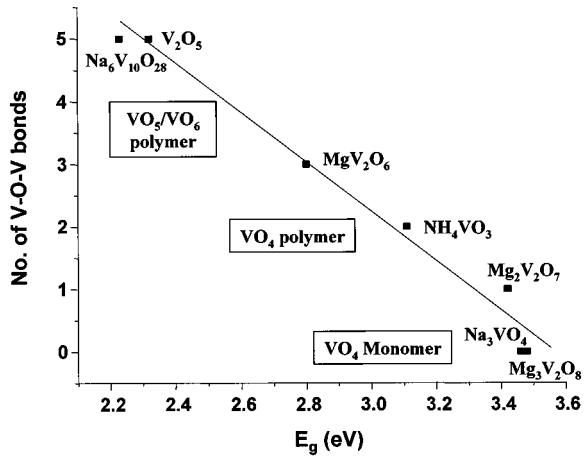

Figure 5. Edge energies of V(V)-containing reference oxides/compounds as a function of number of covalently bonded V−O−V bonds in the coordination sphere of central V(V) cation.

in the coordination sphere of the central V(V) cation (CVB) was established for the reference V(V)-containing oxides/compounds studied, as shown in Figure 5. It was noticed that E_g is inversely proportional to the CVB number. The CVB number is similar to the number of next nearest metal neighbors (N_M) proposed by Weber for Mo compounds,[62] which represents the degree of aggregate/polymerization of the absorbing species. The line shown in Figure 5 can be expressed by the equation of CVB = (14.03−3.95E_g) (±0.34), which is very similar to the correlation obtained by Weber for Mo oxide clusters: N_{Mo} = (16−3.8E_g). The similar correlation obtained for both Mo(VI) and V(V) oxides/compounds suggests a general phenomenon that the edge energies of molecularly sized clusters track with the extent of spatial delocalization of the molecular orbitals involved in the electronic transitions, as proposed by Weber.[62] The isolated VO_4 monomers (CVB = 0) possess the highest edge energies, while the VO_5/VO_6 polymers (CVB = 5) with high spatial delocalization of the molecular orbitals possess the lowest edge energies.

The nature of ligands around the central V(V) cation can also affect its edge energy, and deviations from the linear relationship are observed. As an example, the DRS spectra of V_2O_5 bulk oxide and V_2O_5·x H_2O gel (room-temperature dried, $x \approx 1.8$)[63] are presented in Figure 6. Their local structures are very similar, except the weakly bonded sixth oxygen ligand under V(V) central cation.[64] V_2O_5 bulk oxide consists of two-dimensional layers stacked together through weak bonding between the V(V) atom in the first layer to the oxygen of V═O bond in the second layer. For V_2O_5·1.8 H_2O gel, the two-dimensional layers are separated by the water molecules, and the oxygen in the water molecule serves as the weak sixth ligand for the V(V) cation. According to Sanderson's partial charge calculation,[65] the partial charge on oxygen in H_2O is −0.25, which is more negative than that of O═V group (−0.12) in V_2O_5. Thus, the fact that the change of ligand from V···O═V to V···OH_2 results in a decrease of the edge energy by 0.3 eV may be associated with the low electronegativity (electron-withdrawing) property of oxygen in H_2O as compared to O═V group. As a conclusion, the edge energy is mainly determined by the CVB number/polymerization degree of V(V) cations and is affected to some extent by the nature, such as the electronegativity, of other ligands around the central V(V) cation. Therefore, the edge energy can be used to estimate the local structure of V(V) cations to some extent.

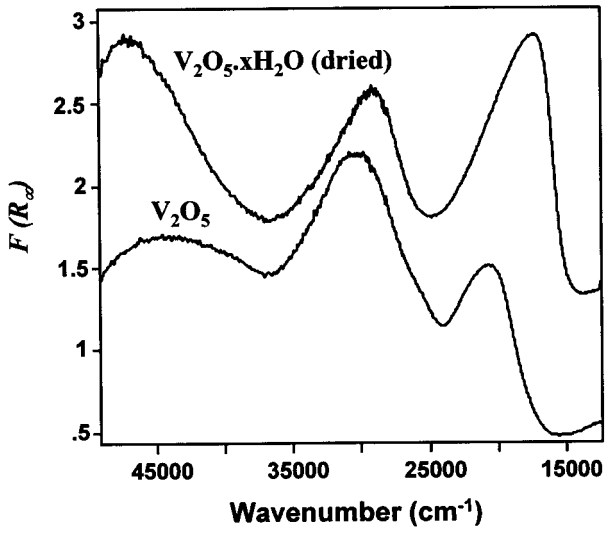

Figure 6. UV−vis DRS spectra of V_2O_5·xH_2O gel and V_2O_5

TABLE 7: Surface Structures of Supported-Vanadia Catalysts under Hydrated and Dehydrated Conditions

sample	E_g (eV)	average CVB number	structural assignments[a]
1% V_2O_5/SiO_2 (hydr.)	2.47	4.27	poly.VO_5/VO_6
1% V_2O_5/SiO_2 (dehy.)	3.60	0	isolated VO_4
12% V_2O_5/SiO_2 (hydr.)	2.46	4.31	poly.VO_5/VO_6
12% V_2O_5/SiO_2 (dehy.)	3.34	0.83	isolated VO_4(d) + V_2O_5 (m)
1% V_2O_5/ZrO_2 (hydr.)	3.48	0	isolated VO_4
1% V_2O_5/ZrO_2 (dehy.)	3.50	0	isolated VO_4
4% V_2O_5/ZrO_2 (hydr.)	2.78	3.05	poly.VO_5/VO_6(d) + poly.VO_4(m)
4% V_2O_5/ZrO_2 (dehy.)	3.13	1.67	poly.VO_4(d) + isolated VO_4(m)
1% V_2O_5/Al_2O_3 (hydr.)	3.88	0	isolated VO_4
1% V_2O_5/Al_2O_3 (dehy.)	3.89	0	isolated VO_4
5% V_2O_5/Al_2O_3 (hydr.)	3.21	1.35	isolated VO_4 + poly.VO_4
5% V_2O_5/Al_2O_3 (dehy.)	3.28	1.07	isolated VO_4 + poly.VO_4
10% V_2O_5/Al_2O_3 (hydr.)	2.86	2.73	poly.VO_4 + poly.VO_5/VO_6
10% V_2O_5/Al_2O_3 (dehy.)	3.02	2.10	poly.VO_4(d)
20% V_2O_5/Al_2O_3 (hydr.)	2.55	3.96	poly.VO_5/VO_6 + poly.VO_4
20% V_2O_5/Al_2O_3 (dehy.)	2.67	3.48	poly.VO_4 + poly.VO_5/VO_6

[a] d − dominant; m − minor.

3. Surface Structures of Supported Vanadium Oxide Catalysts. The correlation of the edge energy to the CVB number indicates that the edge energies of the supported vanadium oxide species can be used for estimating their local structures. The average CVB number for the supported vanadia catalysts is calculated based on the empirical equation obtained above, CVB = (14.03−3.95E_g) (±0.34). The results are listed in Table 7, together with the possible structural assignments. Since the CVB number is the averaged contribution from all the surface vanadium oxide species and the support cation may also affect to some extent the variation in the CVB value due to the ligand effect, it is necessary to discuss this value in association with the structural characterization results obtained by other techniques.

The surface structures of SiO_2-supported vanadia oxide catalysts under hydrated and dehydrated conditions have been discussed in detail in a previous publication.[29a] It was found that in the dehydrated state only isolated VO_4 species are present on the silica surface up to monolayer coverage, whereas the fully hydrated surface vanadium oxide species are proposed to be chain and/or two-dimensional polymers with highly distorted square-pyramidal VO_5 connected by V−OH−V bridges, which resembles the structure of V_2O_5·nH_2O gels. The structural assignments for these samples listed in Table 7 are consistent with the previous conclusion.

For the ZrO_2-supported vanadia catalysts, the structural assignments appear to be straightforward from the average CVB numbers. The 1% V_2O_5/ZrO_2 sample with a surface density of 0.8 V atoms/nm^2 possesses predominantly isolated VO_4 species under both hydrated and dehydrated conditions. However, a LMCT band intensity/feature change was observed during hydration/dehydration, which may be associated with the ligand change between V−O−Zr and V−O−H. The net surface pH at point of zero charge model predicts that hydrated vanadia species at a low loading on ZrO_2 possibly possess a $VO_2(OH)_2$ structure.[47b] The DRS results for the 1% V_2O_5/ZrO_2 sample support the structural change of the surface vanadia species from $VO(O-Zr)_3$ in the dehydrated state to $VO_2(OH)_2$ in the hydrated state.[47a−b] For the 4% V_2O_5/ZrO_2 sample with monolayer coverage of 8.1 V atoms/nm^2, the CVB number for the hydrated sample is 3.05, which may be associated with predominantly polymerized VO_5/VO_6 species with CVB number ranging from 3 to 5. The Raman results showed the presence of decavanadate clusters ($V_{10}O_{28}$) on the zirconia surface at monolayer coverage.[47b] Thus, a small amount of polymerized VO_4 species with a CVB number of 2 may also be present in addition to decavanadate clusters ($V_{10}O_{28}$) with a CVB number of 5, in agreement with the prediction by the point-of-zero-charge model.[47b] However, the average CVB number of 3.05 for the hydrated 4% V_2O_5/ZrO_2 sample suggests that other types of polymerized VO_5/VO_6 species, e.g., the polymerized VO_5/VO_6 species with a CVB number of 3, may also be present. Upon dehydration, the average CVB number of the 4% V_2O_5/ZrO_2 sample decreases markedly to 1.67, which suggests the presence of predominantly polymerized VO_4 species in addition to a small amount of isolated VO_4 species.

For the V_2O_5/Al_2O_3 catalyst system, the edge energy and average CVB number are also a strong function of the vanadia loading, which could be associated with the change in the relative amount of the isolated and polymerized surface vanadium oxide species as well as the change in the polymerization degree of the polymerized species. The 1% V_2O_5/Al_2O_3 sample exhibits remarkably high edge energy of 3.88/3.89 eV under hydrated and dehydrated states due to isolated VO_4 species. This high E_g value compared to other isolated VO_4 structures with edge energy of ∼3.5 eV might be due to the high distortion of the VO_4 structure or the ligand effect. Similar to 1% V_2O_5/ZrO_2, although the edge energy of 1% V_2O_5/Al_2O_3 is almost the same upon hydration/dehydration, the LMCT band intensity/feature is different (see Figure 4), which suggests the ligand change between −O−H and −O−Al. This is consistent with the ^{51}V NMR results[48] and the prediction by the point-of-zero-charge model[47b] that the hydrated 1% V_2O_5/Al_2O_3 sample may possess $VO_3(OH)$ species. For this low loading sample, hydration/dehydration may only affect the local structure of V cations on alumina by changing the relative ratio of V−O−Al to V−O−H. Thus, the DRS results for the 1% V_2O_5/Al_2O_3 sample support the structural change of the surface vanadia species from $VO(O-Al)_3$ in the dehydrated state to $VO_3(OH)$ in the hydrated state.[47a−b] For the hydrated 5% V_2O_5/Al_2O_3 sample, the CVB number of 1.35 indicates the presence of both polymerized VO_4 species and isolated VO_4 species, which is consistent with the prediction of the point-of-zero-charge model[47b] that the polymerized metavanadate $(VO_3)_n$ species coexist with the isolated $VO_3(OH)$ species in the hydrated state. Dehydration decreases the CVB number to 1.07, indicative of the decrease of the amount of the polymerized VO_4 species relative to the isolated VO_4 species. This result suggests that some of the polymerized VO_4 species are dissociated to the isolated VO_4 species after dehydration. The increase of the vanadia loading to 10% V_2O_5 decreases further the edge energy of the surface vanadium oxide species and increases the average CVB number to 2.74 in the hydrated state, suggesting the coexistence of polymerized VO_4 and polymerized VO_5/VO_6 species. This is in good agreement with the Raman results which indicated the presence of polymerized $(VO_3)_n$ and decavanadate ($V_{10}O_{28}$)-like clusters on the hydrated 10% V_2O_5/Al_2O_3 sample.[47b] Dehydration decreases the CVB number to 2.1, which suggests the presence of predominantly polymerized surface VO_4 species with possibly a small amount of polymerized VO_5/VO_6 species. Although the Raman results indicated the presence of isolated VO_4 species,[47a] its amount must be too small to affect the absorption edge of the overall V(V) species. At monolayer coverage of 20% V_2O_5, the CVB number of 3.96 for the hydrated sample suggests the presence of the polymerized VO_5/VO_6 and polymerized VO_4 species since Raman results showed the presence of decavanadate ($V_{10}O_{28}$)-like clusters and the ^{51}V NMR results[48] demonstrated the concurrent presence of octahedral and tetrahedral species. Dehydration decreases the CVB number by ∼0.5, indicating the transformation of some polymerized VO_5/VO_6 species to polymerized VO_4 species. This result is in good agreement with the ^{51}V NMR results[48] that shows the increase of the fraction of tetrahedral V(V) species upon dehydration.

For CeO_2, TiO_2, and Nb_2O_5 supported vanadia catalysts, the edge energies of the surface vanadium oxide species are all below 3.0 eV irrespective of the vanadia loading and environmental conditions. This is because of the possible electronic interaction due to their similar band-gap energies and/or the strong support absorption that overlaps the signal of the surface vanadium oxide species in the same region. In contrast to the expectation and practice by many researchers, the UV−vis DRS spectroscopy may not be able to provide reliable results for the structural assignments of CeO_2, TiO_2, and Nb_2O_5 supported vanadia catalysts.

Conclusions

UV−vis−NIR diffuse reflectance spectroscopy was applied to study the surface structures of molecularly dispersed vanadium(V) oxide on various supports (Al_2O_3, ZrO_2 TiO_2, Nb_2O_5, CeO_2, and SiO_2) under hydrated and dehydrated conditions. The edge energy (E_g) of the LMCT transitions of V(V) cations was found to be excellently correlated with the number of the covalent V−O−V bonds (CVB) around the central V(V) cations. A correlation was established based on some V(V)-reference compounds/oxides: $CVB = 14.03 - 3.95E_g$. For Al_2O_3, ZrO_2, and SiO_2 supports, reliable structural assignments are derived based on this correlation. The results demonstrate that the molecular structures of the surface vanadium oxide species are a strong function of the support, environmental conditions, and the vanadia surface density. Three types of surface vanadium oxide species, i.e., isolated VO_4, polymerized VO_4 and polymerized VO_5/VO_6, may be present, and their relative amount and local structure depend on the above factors. However, for TiO_2, Nb_2O_5, and CeO_2 supported vanadia catalysts, the strong support absorption in the same region as the V(V) cations prevents a reliable determination of the local structure of the surface vanadium oxide species by either the LMCT band position or the edge energy. Interestingly, the effect of regular reflection, which is associated with the relative high concentration of V(V) cations, appears to affect the edge energies of some V(V)-containing materials.

Acknowledgment. This work was supported by the U.S. Department of Energy, Basic Energy Sciences, Grant DE-FG02-93ER14350. The authors thank Dr. Miguel A. Banares for the help with BET measurements and chemical analysis. The authors are grateful for helpful comments by Dr. Bert M. Weckhuysen and Prof. R. A. Schoonheydt.

References and Notes

(1) Arco, M.; Rives, V.; Trujillano, R.; Malet, P. *J. Mater. Chem.* **1996**, *6*, 1419.

(2) Busca, G.; Tittarelli, P.; Tronconi, E.; Forzatti, P. *J. Solid State Chem.* **1987**, *67*, 91. (b) Busca, G.; Centi, G.; Marchetti, L.; Trifiro, F. *Langmuir* **1986**, *2*, 568.

(3) Cavani, F.; Trifiro, F.; Bartolini, A.; Ghisletti, D.; Nalli, M.; Santucci, A. *J. Chem. Soc., Faraday Trans.* **1996**, *92*, 4321.

(4) Corma, A.; Nieto, J. M. N.; Paredes, N. *Appl. Catal. A: General* **1993**, *104*, 161.

(5) Dutoit, D. C. M.; Schneider, M.; Fabrizioli, P.; Baiker, A. *J. Mater. Chem.* **1997**, *7*, 271. (b) Dutoit, D. C. M.; Schneider, M.; Fabrizioli, P.; Baiker, A. *Chem. Mater.* **1996**, *8*, 734.

(6) Morey, M.; Davidson, A.; Eckert, H.; Stucky, G. *Chem. Mater.* **1996**, *8*, 486.

(7) Moshfegh, A. Z.; Ignatiev, A. *Thin Solid Films* **1991**, *198*, 251.

(8) Ramis, G.; Busca, G.; Forzatti, P. *Appl. Catal. B: Environmental* **1992**, *1*, L9.

(9) Grubert, G.; Rathousky, J.; Schulz-Ekloff, G.; Wark, M.; Zukal, A. *Microporous Mesoporous Mater.* **1998**, *22*, 225.

(10) Centi, G.; Perathoner, S.; Trifiro, F.; Aboukais, A.; Aissi, C. F.; Guelton, M. *J. Phys. Chem.* **1992**, *96*, 2617.

(11) Chao, K. J.; Wu, C. N.; Chang, H.; Lee, L. J.; Hu, S.-F. *J. Phys. Chem. B* **1997**, *101*, 6341.

(12) Dzwigaj, S.; Peltre, M. J.; Massiani, P.; Davidson, A.; Che, M.; Sen, T.; Sivasanker, S. *Chem. Commun.* **1998**, 87.

(13) Gontier, S.; Tuel, A. *Microporous Mater.* **1995**, *5*, 161.

(14) Kornatowski, J.; Sychev, M.; Kuzenkov, S.; Strnadova, U.; Pilz, W.; Kassner, D.; Pieper, G.; Baur, W. H. *J. Chem. Soc., Faraday Trans.* **1995**, *91*, 2217. (b) Kornatowski, J.; Wichterlova, B.; Jirkovsky, J.; Löffler, E.; Pilz, W. *J. Chem. Soc., Faraday Trans.* **1996**, *92*, 1067.

(15) Luan, Z.; Xu, J.; He, H.; Klinowski, J.; Kevan, L. *J. Phys. Chem.* **1996**, *100*, 19595. (b) Luan, Z.; Kevan, L. *J. Phys. Chem. B* **1997**, *101*, 2020.

(16) Singh, P. S.; Bandyopadhyay, R.; Rao, B. S. *J. Mol. Catal. A: Chemical* **1995**, *104*, 103.

(17) Wark, M.; Koch, M.; Brückner, A.; Grünert, W. *J. Chem. Soc., Faraday Trans.* **1998**, *94*, 2033. (b) Wark, M.; Brückner, A.; Liese, T.; Grünert, W. *J. Catal.* **1998**, *175*, 48.

(18) Wei, D.; Wang, H.; Feng, X.; Chueh, W.-T.; Ravikovitch, P.; Lyubovsky, M.; Li, C.; Takeguchi, T.; Haller, G. L. *J. Phys. Chem. B* **1999**, *103*, 2113.

(19) Catana, G.; Rao, R. R.; Weckhuysen, B. M.; Van Der Voort, P.; Vansant, E.; Schoonheydt, R. A. *J. Phys. Chem. B* **1998**, *102*, 8005. (b) Weckhuysen, B. M.; Schoonheydt, R. A. *Catal. Today* **1999**, *49*, 441.

(20) Aguilar Cruz, A. M.; Eon, J. G. *Appl. Catal. A: General* **1998**, *167*, 203.

(21) Alemany, L. J.; Lietti, L.; Ferlazzo, N.; Forzatti, P.; Busca, G.; Giamello, E.; Bregani, F. *J. Catal.* **1995**, *155*, 117. (b) Alemany, L. J.; Jimenez, M. C.; Pardo, E.; Machek, J.; Svachula, S. *React. Kinet. Catal. Lett.* **1993**, *51*, 383.

(22) Arena, F.; Frusteri, F.; Martra, G.; Coluccia, S.; Parmaliana, A. *J. Chem. Soc., Fraday Trans.* **1997**, *93*, 3849.

(23) Bañares, M. A.; Alemany, L. J.; Jimenez, M. C.; Larrubia, M. A.; Delgado, F.; Cranados, M. L.; Martinez-Arias, A.; Blasco, J. M.; Fierro, J. L. *J. Solid State Chem.* **1996**, *124*, 69.

(24) Blasco, T.; Concepcion, P.; Nieto, J. M. L.; Perez-Pariente, J. *J. Catal.* **1995**, *152*, 1.

(25) Ciambelli, P.; Lisi, L.; Russo, G.; Volta, J. C. *Appl. Catal. B: Environmental* **1995**, *7*, 1.

(26) Dall'Acqua, L.; Baricco, M.; Berti, F.; Lietti, L.; Giamello, E. *J. Mater. Chem.* **1998**, *8*, 1441.

(27) Eon, J. G.; Olier, R.; Volta, J. C. *J. Catal.* **1994**, *145*, 318. (b) Abdelouahab, F. B.; Olier, R.; Ziyad, M.; Volta, J. C. *J. Catal.* **1995**, *157*, 687.

(28) Fountzoula, G.; Matralis, H. K.; Papadopoulou, Ch.; Voyiatzis, G. A.; Kordulis, Ch. *J. Catal.* **1999**, *184*, 5.

(29) Gao, X.; Bare, S. R.; Weckhuysen, B. M.; Wachs, I. E. *J. Phys. Chem. B* **1998**, *102*, 10842. (b) Gao, X.; Bare, S. R.; Fierro, J. L. G.; Wachs, I. E. *J. Phys. Chem. B* **1999**, *103*, 618. (c) Gao, X.; Fierro, J. L. G.; Wachs, I. E. *Langmuir* **1999**, *15*, 3169.

(30) Gervasini, A.; Fornasari, G.; Bellussi, G. *Appl. Catal. A: General* **1992**, *83*, 235.

(31) Hausinger, G.; Schmelz, H.; Knözinger, H. *Appl. Catal.* **1988**, *39*, 267.

(32) Inomata, M.; Mori, K.; Miyamoto, A.; Ui, T.; Murakami, Y. *J. Phys. Chem.* **1983**, *87*, 754. (b) Inomata, M.; Mori, K.; Miyamoto, A.; Murakami, Y. *J. Phys. Chem.* **1983**, *87*, 761.

(33) Jonson, B.; Rebenstorf, B.; Larsson, R.; Andersson, S. L. T. *J. Chem. Soc., Faraday Trans. 1* **1988**, *84*, 1897. (b) Jonson, B.; Rebenstorf, B.; Larsson, R.; Andersson, S. L. T.; Lundin, S. T. *J. Chem. Soc., Faraday Trans. 1* **1986**, *82*, 767.

(34) Kantcheva, M. M.; Hadjiivanov, K. I.; Klissurski, D. G. *J. Catal.* **1992**, *134*, 299.

(35) Khodakov, A.; Yang, J.; Su, S.; Iglesia, E.; Bell, A. T. *J. Catal.* **1998**, *177*, 343. (b) Khodakov, A.; Olthof, B.; Bell, A. T.; Iglesia, E. *J. Catal.* **1999**, *181*, 205.

(36) Lischke, G.; Hanke, W.; Jerschkewitz, H.-G.; Öhlmann, G. *J. Catal.* **1985**, *91*, 54.

(37) Prinetto, F.; Ghiotti, G.; Occhiuzzi, M.; Indovina, V. *J. Phys. Chem. B* **1998**, *102*, 10316.

(38) Rajadhyaksha, R. A.; Hausinger, G.; Zeilinger, H.; Ramstetter, A.; Schmelz, H.; Knözinger, H. *Appl. Catal.* **1989**, *51*, 67.

(39) Reddy, B. M.; Chowdhury, B.; Ganesh, I.; Reddy, E. P.; Rojas, T. C.; Fernández, A. *J. Phys. Chem. B* **1998**, *102*, 10176. (b) Reddy, J. S.; Liu, P.; Sayari, A. *Appl. Catal. A: General* **1996**, *148*, 7.

(40) Scharf, U.; Schraml-Marth, M.; Wokaun, A.; Baiker, A. *J. Chem. Soc., Faraday Trans.* **1991**, *87*, 3299. (b) Schraml-Marth, M.; Wokaun, A.; Pohl, M.; Krauss, H.-L. *J. Chem. Soc., Faraday Trans.* **1991**, *87*, 2635. (c) Schraml-Marth, M.; Wokaun, A.; Baiker, A. *Fresenius J. Anal. Chem.* **1991**, *341*, 87.

(41) Van Der Voort, P.; Babitch, I. V.; Grobet, P. J.; Verberckmoes, A. A.; Vansant, E. F. *J. Chem. Soc., Faraday Trans.* **1996**, *92*, 3635. (b) Van Der Voort, P.; White, M. G.; Mitchell, M. B.; Verberckmoes, A. A.; Vansant, E. F. *Spectrochim. Acta, Part A* **1997**, *53*, 2181.

(42) Lever, A. B. P. *Inorganic Electronic Spectroscopy*; Elsevier: New York, 1968.

(43) Kortum, G.; Braun, W.; Herzog, G. *Angew. Chem., Int. Ed. Engl.* **1963**, *2*, 333.

(44) Delgass, W. N.; Haller, G. L.; Kellerman, R.; Lunsford, J. H. *Spectroscopy in Heterogeneous Catalysis*; Academic Press: New York, 1979; p 86.

(45) Klier, K. *Catal. Rev.* **1967**, *1*, 207.

(46) Tandon, S. P.; Gupta, J. P. *Phys. Stat. Sol.* **1970**, *38*, 363.

(47) Deo, G.; Wachs, I. E.; Haber, J. *Crit. Rev. Surf. Chem.* **1994**, *4*, 141. (b) Deo, G.; Wachs, I. E. *J. Phys. Chem.* **1991**, *95*, 5889. (c) Deo, G.; Wachs, I. E. *J. Catal.* **1994**, *146*, 323. (d) Wachs, I. E.; Weckhuysen, B. M. *Appl. Catal. A: General* **1997**, *157*, 67.

(48) Eckert, H.; Wachs, I. E. *J. Phys. Chem.* **1989**, *93*, 6796.

(49) Ruitenbeek, M. Ph.D. Thesis, Universiteit Utrecht, The Netherlands, 1999.

(50) Dimitrov, V.; Sakka, S. *J. Appl. Phys.* **1996**, *79*, 1736.

(51) Lebouteiller, A.; Courtine, P. *J. Solid State Chem.* **1998**, *137*, 94.

(52) Davis, E. A.; Mott, N. F. *Philos. Mag.* **1970**, *22*, 903.

(53) Hossein, A. A.; Hogarth, C. A.; Beynon, J. *J. Mater. Sci. Lett.* **1994**, *13*, 1144.

(54) Khan, G. A.; Hogarth, C. A. *J. Mater. Sci. Lett.* **1991**, *26*, 412.

(55) Tauc, J.; Grigorovici, R.; Vancu, A. *Phys. Stat. Sol.* **1966**, *15*, 627. (b) Tauc, J. In *Optical Properties of Solids*; Abeles, F., Ed.; North-Holland: New York, 1972.

(56) Karvaly, B.; Hevesi, I. *Z. Naturforsch. Teil A* **1971**, *26*, 363.

(57) Mokerov, W. G.; Rakov, A. V. *Sov. Phys. Solid State* **1969**, *11*, 150.

(58) Conlon, D. C.; Doyle, W. P. *J. Chem. Phys.* **1961**, *35*, 752.

(59) Kenny, N.; Kannewurf, C. R.; Withmore, D. H. *J. Phys. Chem. Sol.* **1966**, *27*, 1237.

(60) Hevesi, I. *Acta Phys. Hung.* **1967**, *23*, 415.

(61) Gao, X.; Bare, S. R.; Fierro, J. L. G.; Banares, M. A.; Wachs, I. E. *J. Phys. Chem. B* **1998**, *102*, 5653.

(62) Weber, R. S. *J. Catal.* **1995**, *151*, 470.

(63) Livage, J. *Chem. Mater.* **1991**, *3*, 578.

(64) Stizza, S.; Mancini, G.; Benfatto, M.; Natoli, C. R.; Garcia, J.; Bianconi, A. *Phys. Rev. B* **1989**, *40*, 12229.

(65) Sanderson, R. T. *J. Chem. Educ.* **1988**, *65*, 112. (b) Sanderson, R. T. *J. Chem. Educ.* **1988**, *65*, 227.